Explaining cold-water coral community assembly with seabed and hydrodynamic features

Siluo Chen (6514030)

Utrecht University

Royal Netherlands Institute for Sea Research

Supervisors Max Rietkerk   Utrecht University

Anna van der Kaaden   Royal Netherlands Institute for Sea Research

Evert de Froe   Royal Netherlands Institute for Sea Research

Abstract

Cold-water coral reefs, serving as biodiversity hotspots in the deep sea, can form into carbonate mounds, which are important oceanographic structures with great ecological values. Reef-forming corals and their associated community can display different distribution patterns between mounds, which are hypothesized to be governed by the interactions between the reef community and the environment, i.e. seabed topography and hydrodynamics. In this study, we aimed to investigate the spatial variation of the cold-water coral community distribution, including the inter-mound and intra-mound variation, and explain the community distribution with seabed topographical and hydrodynamic variables. Community assembly data was acquired from remotely operated vehicle (ROV) videos; topographical variables were calculated from multi-beam map, and hydrodynamic variables were extracted from model outputs. Two multivariate statistical analyses, between-class analysis (BCA) and co-inertia analysis were applied to investigate the inter-mound and intra-mound variation of reef community, and the relationship between topographical and hydrodynamic variables and reef community data, respectively. Our results show that community generally concentrates at the summit of smaller mounds, while at the upper flank of larger mounds, implying a potential of vertical growth for small mounds and a steady state of that for larger mounds; endemism was observed on mound scale; reef-forming corals, zoanthids, black corals Antipatharia, and soft corals Alcyonacea are associated with bathymetric position index (BPI), but have no correlation or negative correlation with current speed, implying that these faunal groups cannot effectively capture food particles in high-speed ambient currents; demosponges are positively correlated with slope steepness and horizontal current speed, implying that they use current-induced waterflows to save energy. To further provide insights regarding cold-water coral reef ecosystems, regional-scale biochemistry related to cold-water coral reef and the niche studies of mound-scale endemic species are suggested for the future research.

Acknowledgement

I hereby express my sincere gratefulness to my supervisors Anna van der Kaaden, Evert de Froe, and Max Rietkerk, for their kindness, patience, and professionalism throughout their supervision. They are not only supervisors, but also friends, providing me help in personal life through the hard time. Also, I am sincerely grateful to Sandra Maier and Dick van Oevelen, who are not officially my supervisors, but also provided me a lot of inspiring advice and encouragement.

Meanwhile, many thanks to my parents who have been supporting me financially and mentally all along, to my ex-girlfriend Jessie who has provided love and support for more than 90% of my thesis period, to my friends in De Keete and volleyball club Bok, who have been giving me so much joy during spare time.

Contents

1 Introduction

Among the known coral species, over half of them occur in deep and/or cold water, where the coral thickets can form into reef structures and further into larger mound-like structures. These coral-capped carbonate mounds are key oceanographic structures, providing habitats for a large assembly of cold-water coral associated fauna (Roberts et al., 2009). However, how the environment influences the reef composition and how cold-water coral reef communities differ between mounds remain unclear.

The interaction between reef-forming coral assembly and mound structure has been studied extensively (e.g., Davies et al., 2011; Mohn et al., 2014; Morgan et al., 2019). Two generally accepted theories on these interactions are "environmental control theory" and "ecosystem engineer control theory" (Roberts et al., 2009; Soetaert et al., 2016). The "environmental control theory" refers to that animals require optimal environmental conditions to thrive, which is in the case of cold-water corals: a suitable flow regime, temperature ranging from 4 °C to 14 °C, salinity ranging from 34.9 to 35.5, water depth ranging from roughly 200 meters to 1500 meters, and aragonite saturation state (Roberts et al., 2009; Freiwald, 2011). However, animals are not solely determined by environmental factors, but they can also modify their local environment, creating a two-way interaction. Therefore, the "ecosystem engineer control theory" that builds on the "environmental control theory" stresses that based on these optimal environmental conditions, cold-water corals may modify the environment by forming complex three-dimensional structures and large carbonate mounds, in order to enhance and retain nourishment from their surroundings (Cacchione et al., 2002; Soetaert et al., 2016). Since species may influence each other indirectly through their effect on the environment, on top of direct interactions, the causality between environmental factors and cold-water coral reef community is complex and so far unclear. In this study, we aim to investigate we aim to investigate this intricate linkage between community composition and environmental factors.

Here, the cold-water coral community refers to the benthic megafauna that occur

in cold-water coral reef ecosystems. Reef-forming corals are ecosystem engineers (Jones et al., 1994). The reef frameworks they form are of high heterogeneity and complexity (Roberts et al., 2009). The framework serves as habitats for other organisms, concretely as inhabitation, refuge, and foraging site. Non-reef-forming corals, including soft corals Alcyonacea and black corals Antipatharia are important faunal groups. They can occur with highly diverse aggregation, and they can also form habitats, which is known as "coral garden" (Roberts et al., 2009). Sponges are another important taxon. They can accelerate nutrient cycling through the so-called "sponge loop", in which they take up dissolved organic matter (DOM) released within coral mucus, and produce particulate organic matter (POM) by shedding their cells with a high cell turnover, serving as the food for detritivores at higher trophic level (De Goeij et al., 2013; Rix et al., 2016). Besides the "sponge loop" function, sponges can also serve as bioeroders, degrading the dead framework into coral rubbles leading to renewed larvae settlement (Freiwald, 2002). Other faunal groups related to cold-water coral community include zoanthids, crinoids, and sea urchins.

The occurrence of cold-water corals on the carbonate mound is in close relationship with the mound dynamics. Cyr et al. (2016) hypothesized an interrelationship between the spatial distribution of cold-water corals on a mound and the mound size. They found that Haas mound, a relatively large carbonate mound at Rockall area in the Northeast Atlantic with approximately 300 meters height, had no waterflows nourishing the summit neither from the surface nor from the deep, leading to very limited cold-water coral and associated community distribution at its summit; therefore, they hypothesized that Haas mound has reached a steady state in height. Furthermore, they found that waterflows were able to wash over the summits of smaller mounds, hypothesizing that this would enable the growth of cold-water corals and the subsequent vertical growth of those mounds. The study by Cyr et al. (2016) implies a spatial variation of cold-water coral community distribution, which can be both intra-mound and inter-mound, referring to that the species can be densely distributed at certain zones of a mound, forming a distribution pattern, whereas such pattern can vary between mounds.

According to the "environmental control theory", such spatial variation of cold-water coral community distribution is governed by environmental factors.

Environmental variables that affect coral reef community assembly

Environmental factors shaping the variation in community assembly include seabed topography, hydrodynamics. Seabed topography is described by the following features: (1) slope, (2) orientation, (3) curvature and relative position of features, and (4) terrain variability (Wilson et al., 2007). Slope may affect community assembly, because it plays a key role in affecting the velocity of vertical currents that transport organic matter from the surface photic zone to the deep water as well as forming trapped waves that retain the organic matter (Soetaert et al. 2016; Kunze & Smith, 2004). Orientation can explain biomass and community assembly variation, because communities present on slopes that encounters the benthic currents are likely to receive more food, and therefore show increased diversity and biomass (Gage & Tyler, 1991).

Curvature describes the change rate of the slope and is denoted as bathymetric position index (BPI) (Weiss, 2001; Iampietro & Kvitek, 2002; Lundblad et al., 2006). There have been numerous studies that included BPI as a seabed topographical indicator, and though they agreed that BPI largely explained the live coral coverage variation, their conclusions regarding the impact of BPI were different (Dolan et al., 2008; Guinan et al., 2009; De Clippele et al., 2017). Concretely, Dolan et al. (2008) postulated that there should be an optimal BPI for cold-water coral assembly, while Guinan et al. (2009) and De Clippele et al. (2017) concluded that the relationship between BPI and cold-water coral assembly should be linearly positive Therefore, further research on how BPI affect the cold-water coral community assembly is still required. For terrain variability, rugosity serves as one of the most comprehensive and commonly used indicators (Wilson et al., 2007). It is quantitatively defined as the ratio of the surface area to the planar area and been found positively correlated to the local biodiversity.

Higher rugosity implies higher structural complexity and therefore tends to create more niches (Dustan et al., 2013).

Indicators that describe the hydrodynamics include velocity and direction. High current speed is often associated with healthy cold-water corals; internal tidal currents transport food to cold-water corals and their associated community, while benthic currents prevents cold-water corals from sedimentation (Mienis et al., 2007). The downwelling and upwelling are also important food transport mechanisms for the cold-water coral community, as downwelling has been found to transport organic matter from the surface production and upwelling can bring about the resuspension of benthic organic matter (Davies et al., 2009).

Research questions

In summary, cold-water coral community assembly shows variation within a coral mound and between coral mounds, and such variation is governed by hydrodynamics and seabed topography, whereas cold-water corals can alter the local topography and further modifying the hydrodynamics in their favor, e.g. the formation of trapped waves and/or the acceleration of downwelling (Kunze & Smith, 2004; Soetaert et al., 2016). In this study, we combine video analysis of cold-water coral community on several carbonate mounds with topographical data and hydrodynamic model output to investigate the spatial variation of cold-water coral community distribution and its relationship with seabed topography and hydrodynamics. The main research question is: *what is the impact of hydrodynamics and seabed topography on benthic community assembly?* This will be divided into sub-questions: (1) *What are the inter-mound and intra-mound variation of cold-water coral community assembly?* (2) *What topographical and hydrodynamic features can affect the spatial variation of cold-water coral community assembly?* Through this research, we hope to shed light on the conservation of deep-sea environment and ecosystems under the climate change.

2 Materials and Methods

2.1 Study site

Video transect data has been collected from Rockall Bank (Roberts & shipboard party, 2013). The bank is located at the west of Ireland and has long been a hotspot for cold-water coral studies (Kenyon et al., 2003). The Scleractinia *Lophelia pertusa* (Linnaeus, 1758) and *Madrepora oculata* (Linnaeus, 1758) are the major reef-forming coral species there. The corals located in the southern Rockall Trough, where the video transects were taken, have mainly been found on carbonate mounds at depths between 600 meters to 800 meters (Van Weering et al. 2003).
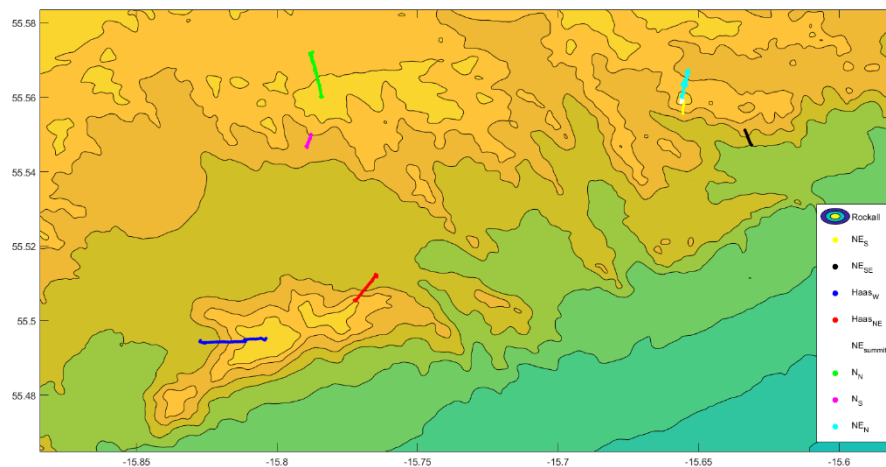

Figure 1. Map of the transects that were taken at three mounds, which are Haas mound (at the bottom of the figure), North mound (to the north of Haas mound), and Northeast mound (to the northeast of Haas mound) which are along the southern flank of Northeast mound. The transects were taken along the southern flank of Northeast mound (NE_S), the southeastern flank of Northeast mound (NE_{SE}), the western flank of Haas mound ($Haas_W$), the northeastern flank of Haas mound ($Haas_{NE}$), the summit of Northeast mound (NE_{summit}), the northern flank of North mound (N_N), the southern flank of North mound (N_S), and the northern flank of Northeast mound (NE_N).

Table 1. Information of the transects

Transects	Side	Start latitude (°N)	End latitude (°N)	Start longitude (°W)	End longitude (°W)
NE$_S$	Southern flank	55.55563	55.559154	15.65569	15.655764
NE$_{SE}$	Southern flank	55.54742	55.55131	15.6314	15.6336
Haas$_W$	Western flank	55.49468	55.49533	15.8272	15.8039
Haas$_{NE}$	Northeastern flank	55.5125	55.5053	15,765	15.7723
NE$_{summit}$	Southern flank	55.55941	55.5601	15.656	15.6556
N$_N$	Northern flank	55.57183	55.56	15.7884	15.7843
N$_S$	Southern flank	55.54686	55.55021	15.7898	15.7879
NE$_N$	Northern flank	55.56712	55.56002	15.654	15.6557

2.2 Video data

Video data in this survey originates from remotely operated vehicles (ROV) by Roberts & shipboard party (2013). The ROV-video dataset was collected on board with the *Holland 1 ROV*, installed with a Reson 7125 multibeam system and a downward-facing High-Definition (HD) camera mounted on its bottom. Data recording was done via the Reson software PDS2000 and supported by the inputs of the ROV depth sensor and USBL navigation. The ROV recorded downward-facing HD video during a series of transects covering the entire surface of the mound. To maintain a clear image of the mound surface, the ROV was flown < 2 m above the mound surface at a survey speed of < 2 knots (cruise number JC073: Roberts & shipboard party, 2013).

Eight transects taken at three mounds (Figure 1) were acquired from Dr. Laurence de Clippele. Detailed information of each dive is provided in table 1. The video data

was transformed into layers of images using Photoshop, and every one out of 500 frames were extracted from each video transect. Megafauna in the images were classified into 13 groups, including (1) reef-forming live corals (i.e. Scleractinia and stylasterids), (2) soft corals, (3) dead framework, (4) demosponges, (5) glass sponges, (6) zoanthids, (7) sea urchins, (8) hydrozoans, (9) sea star *Porania*, (10) crinoids, (11) black corals, (12) crustaceans, and (13) sea cucumbers. The coverage in percentage of these groups in each image layer was then calculated through MATLAB.

Starting from the first layer of the extracted ones, around one out of 20 layers were labelled. When a layer was not suitable for labelling, the clearest image was selected from five adjacent frames based onclearness, scope, and biomass richness,. In total, I collected 198 labelled images, which were further divided into four zones—summit, upper flank, lower flank, and off-mound area, according to the position of the layer. The positions were determined through the relative position index (RPI), which was calculated as:

$$RPI = \frac{layer\ altitude - mound\ foot\ altitude}{mound\ top\ altitude - mound\ foot\ altitude}$$

The altitudes of mound top and mound foot were determined specifically for each mound. The zonation based on RPI is described in table 2.

Table 2. Zonation based on RPI

PI value	$0.85 < PI$	$0.55 < PI \leq 0.85$	$0 < PI \leq 0.55$	$PI \leq 0$
Zonation	Summit	Upper flank	Lower flank	Off-mound

2.3 Topographic features

Terrain parameters used were (1) slope, (2) orientation, (3) curvature and relative position of features, and (4) rugosity (Wilson et al., 2007). The scale of the features,

except of the terrain viability, is a 50-meter-by-50-meter grid cell. The feature is calculated from its two neighboring cells to the south and east, and itself. Slope is the first derivative of topography, and the slope at grid cell (i, j) was calculated as:

$$S^{(i,j)} = \sqrt{\left[S_x^{(i,j)}\right]^2 + \left[S_y^{(i,j)}\right]^2}$$

Where

$$S_x^{(i,j)} = \frac{Z^{(i,j+1)} - Z^{(i,j)}}{l_x}$$

And

$$S_y^{(i,j)} = \frac{Z^{(i+1,j)} - Z^{(i,j)}}{l_y}$$

Here, the slope S is decomposed into the slope along east-west S_x and the slope along south-north S_y. Z denotes the bathymetric value of the grid cell; l_x and l_y denote the lengths of the grid cell in latitude and longitude, respectively. It is notable that for the convenience of linear algebra calculation in MATLAB, i denotes the grid cell on y-axis, that is, longitude, and j denotes the grid cell on x-axis, that is, latitude.

Orientation is defined as the azimuthal direction of the slope and is further decomposed into eastness and northness, which are defined as the degree at which the slope faces east and north, respectively. The calculation of eastness and northness at grid cell (i, j) was given by Wilson et al. (2007):

$$A^{(i,j)} = \arctan\left(\frac{S_y^{(i,j)}}{S_x^{(i,j)}}\right)$$

$$eastness^{(i,j)} = \sin\left(A^{(i,j)}\right)$$

$$northness^{(i,j)} = \cos\left(A^{(i,j)}\right)$$

Here, A refers to the azimuth of the slope. If $eastness = 1$, then the slope faces entirely to the east; if $eastness = -1$, then then slope faces entirely to the west. These apply the same way to northness.

Bathymetric position index (BPI), the second-order derivative of slope, is a major indicator that interprets the curvature and relative position of features (Weiss, 2001; Iampietro & Kvitek, 2002; Lundblad et al., 2006). The BPI at grid cell (i, j) was calculated as:

$$BPI^{(i,j)} = \sqrt{\left[BPI_x^{(i,j)}\right]^2 + \left[BPI_y^{(i,j)}\right]^2}$$

Where

$$BPI_x^{(i,j)} = \frac{S^{(i,j+1)} - S^{(i,j)}}{l_x}$$

And

$$BPI_y^{(i,j)} = \frac{S^{(i+1,j)} - S^{(i,j)}}{l_y}$$

Rugosity is a major indicator that describes the roughness of the surface. High rugosity is usually associated with high biodiversity because more niches tends to be created with higher structural complexity (Dustan et al., 2013). Because the resolution of the bathymetric map (50 m) is too high to calculate rugosity, I estimated the rugosity directly from the ROV videos using a habitat assessment score. In which rugosity is assigned with an integer score from one to five, among which one refers to simply flat seabed, and five refers to seabed with high terrain viability. The detail of the HAS system is elaborated by Gratwicke and Speight et al. (2005).

Hydrodynamics

Hydrodynamic data was acquired from the model output of van der Kaaden (Van der Kaaden et al., pers. comm.). They simulated the average benthic current velocity of February and August, respectively, within 120 time-steps of 6 hours. The modeled velocity was decomposed into three dimensions—the value along the x-axis, u, the value along the y-axis, v, and the value along the vertical axis, w.

Table 3. Variables, methods, and data sources in co-inertia analysis

	Analysis	Variables	Method & source
Environmental data	Hill-Smith analysis	Slope	Calculation from multi-beam data
		Eastness	
		Northness	
		BPI	
		Rugosity	Estimation from ROV data
		framework coverage	Calculation from ROV data
		Sediment coverage	
		u	Model outputs Van der Kaaden (pers. comm)
		v	
		w	
Species data	Principal component analysis	Live Scleractinia	Calculation from ROV data
		Other live corals	
		Demosponges	
		Glass sponges	
		Zoanthids	
		Sea urchins	
		Hydrozoans	
		Sea star *Porania*	
		Crinoids	
		Fish	
		Crustaceans	

Statistical analysis

The intra-mound and inter-mound community assembly spatial variation is studied via between-class analysis (BCA) using program R (RC Team, 2019). BCA is a supervised group analysis that is based on a feature projection technique, which, in this study,

would be the principle component analysis (PCA). The scores of variables calculated by PCA would be divided into groups through a supervised method, and BCA further project the coordinate system in a way that maximizes the variation of group means (Chessel et al., 2004). With BCA, the overall assembly variation between different zones and the zone-specific assembly variation between different mounds were tested.

To further investigate the relationship between the environmental variables and the spatial pattern of cold-water coral community assembly, co-inertia analysis was applied (Table 3). Aiming to reveal the concordance in structure of the species data and the environmental data, co-inertia analysis combines the ordinations of environmental variable dataset and community dataset into one analysis, and thus investigating the linear combination of these two datasets that leads to the maximal concordance. By doing so, co-inertia analysis gives us insight into the correlation between the environment and the species. For the feature projection of two datasets, PCA was applied on species dataset, and because environmental dataset contained both measured values and nominal values (i.e. rugosity), Hill-Smith analysis was applied on this dataset (Thioulouse et al., 2018).

3   Results

3.1   Community assembly

The detailed community assembly, biodiversity, and environmental information of each zone (off-mound, lower flank, upper flank, or summit) and transect are depicted in figure 2 to figure 9.
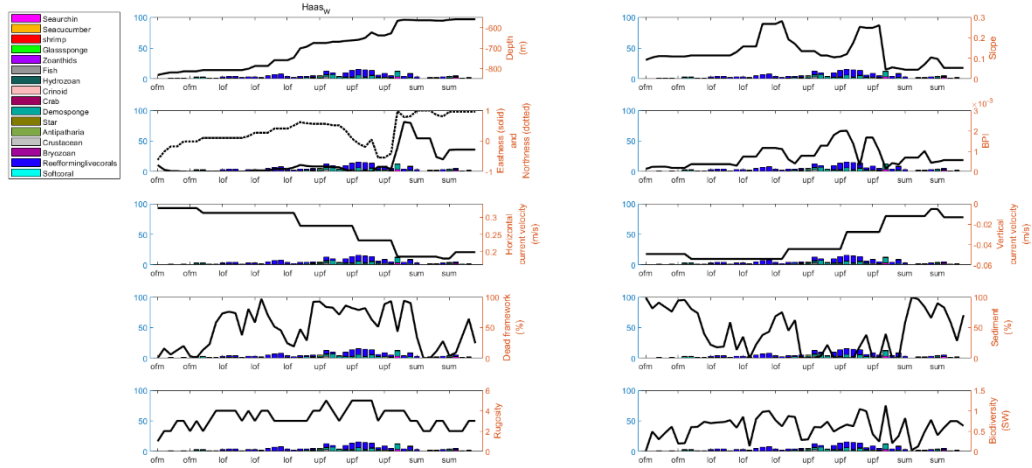
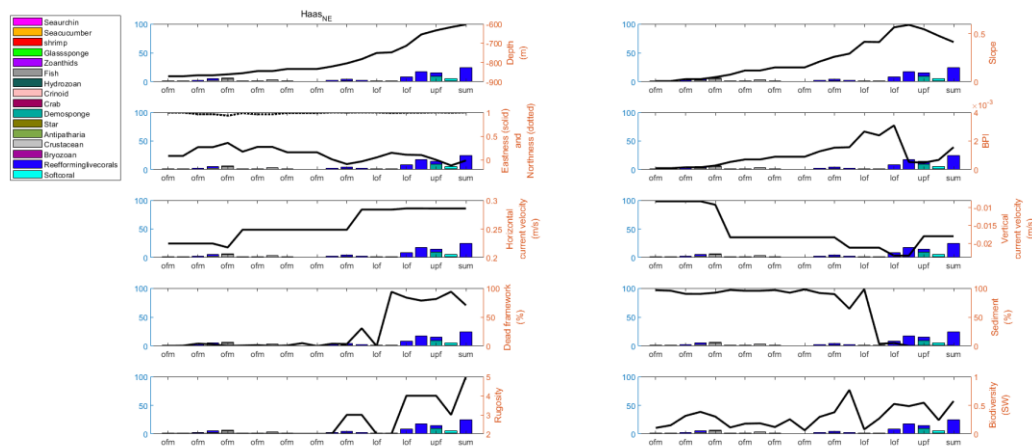**Figure 2.** The community assembly and environmental conditions of the transect along the western flank of Haas mound. The x-axis refers to the zones, i.e. the off-mound area (ofm), the lower flank (lof), the upper flank (upf), and the summit (sum). The y-axis on the left refers to the coverage of detected faunal group in percentage. The y-axis on the right refers to the values of environmental variables, including depth, slope angle, orientation, BPI, horizontal and vertical current velocity, dead framework coverage, sediment exposure, rugosity, and biodiversity described in Shannon-Wiener index.

Figure 3. The community assembly and environmental conditions of the transect along the northeastern flank of Haas mound. Information regarding the x-axis and y-axis are the same as in figure 2.

On Haas mound, both the two transects along the western flank and northeastern flank respectively, have relatively dense reef-forming live coral and demosponge coverage at the upper flank and barren live organism distributed at the lower flank and the off-mound area (figure 2 and figure 3). The maximal reef-forming live coral and demosponge coverage are 24% and 9% respectively. The corresponding environmental features of high reef-forming live coral and demosponge coverage, however, are not consistent between these two flanks, except for high rugosity (≥ 4), high dead framework coverage ($> 50\%$) and low sediment exposure ($< 50\%$). Along the western flank, these environmental features include relatively high BPI at approximately 0.002, horizontal current velocity around 0.25 m/s, and downwelling velocity around 0.04 m/s. Along the northeastern flank, these environmental features include large slope angle above 0.4, BPI below 0.002 which is low compared to that along the western flank, comparably high horizontal current velocity around 0.28 m/s, and comparably low downwelling velocity around 0.02 m/s.
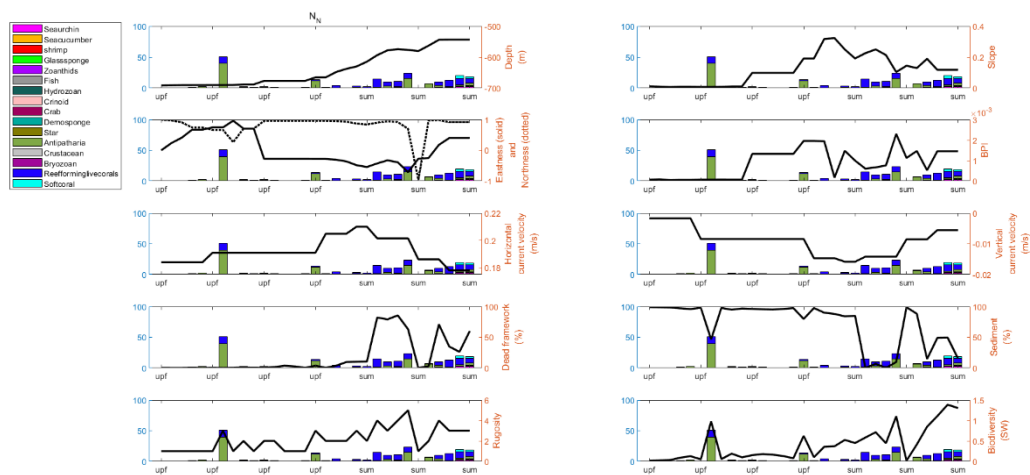

Figure 4. The community assembly and environmental conditions of the transect along the northern flank of North mound. Information regarding the x-axis and y-axis are the same as in figure 2.
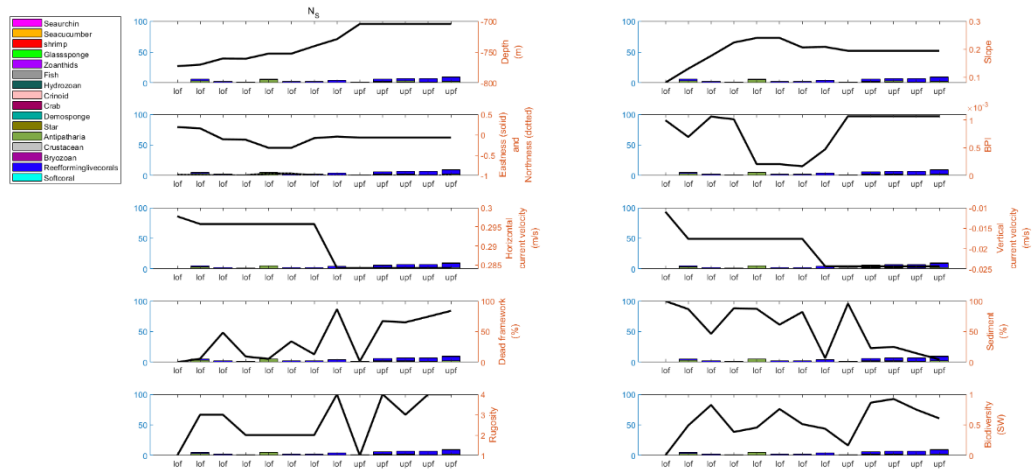
Figure 5. The community assembly and environmental conditions of the transect along the southern flank of North mound. Information regarding the x-axis and y-axis are the same as in figure 2.

The community composition along the southern flank and northern flank of North mound are similar, with mainly reef-forming live corals and black corals Antipatharia distributed and a comparably small amount of soft corals Alcyonacea occurring at two sites on the summit (figure 4 and figure 5). Compared to the community assembly on Haas mound, the community assembly on North mound does not include demosponges, whereas black corals Antipatharia and soft corals Alcyonacea are endemic. Reef-forming corals, apart from their dense distribution at upper flank on Haas mound, concentrate at the summit of North mound, where black corals Antipatharia and soft corals Alcyonacea occurrences are also witnessed. The southern flank and northern flank of North mound, however, display different community assembly distribution. The southern flank is characterized by large area of bare land at the upper flank, with dense black corals Antipatharia at only one site and little framework coverage. The northern flank contains richer framework and live organism coverage, with reef-forming live corals occurring on both the lower flank and upper flank, though less than that on the summit.

Similar with the transects on Haas mound, transects on North mound also shows

high association between relatively high reef-forming live coral coverage and high dead framework coverage, low sediment exposure, high rugosity, and high biodiversity. Figure 4 displays two reef-forming live coral patches at the summit of North mound. The slope angle at these two patches varies from approximately 0.1 to above 0.2, and the BPI varies from approximately 0.0005 to above 0.002. The horizontal current velocity and downwelling velocity at the patch closer to the upper flank are around 0.2 m/s and 0.015 m/s respectively, both higher than those at the other patch, which are around 0.18 m/s and 0.007m/s respectively. Figure 5 shows that on the upper southern flank of North mound where live organism coverage is relatively rich along the flank, the slope angle, the BPI, the horizontal current velocity, and the downwelling velocity are consistent, with approximately 0.2, 0.001, 0.285 m/s, and 0.025 m/s respectively.
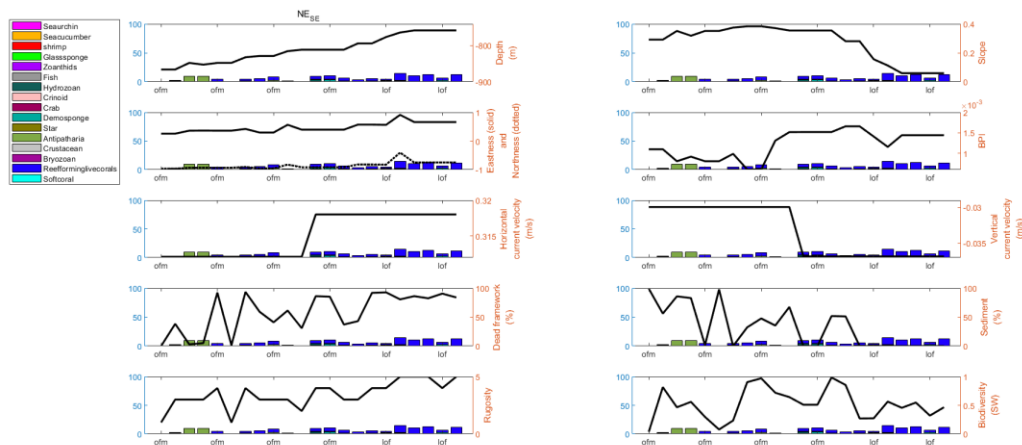

Figure 6. The community assembly and environmental conditions of the transect along the southeastern flank of Northeast mound. Information regarding the x-axis and y-axis are the same as in figure 2.
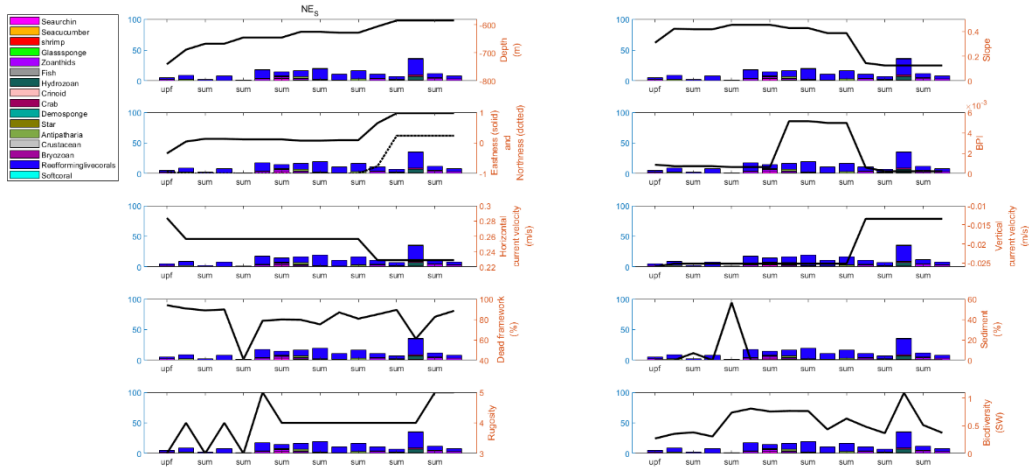
Figure 7. The community assembly and environmental conditions of the transect along the southern flank of Northeast mound. Information regarding the x-axis and y-axis are the same as in figure 2.
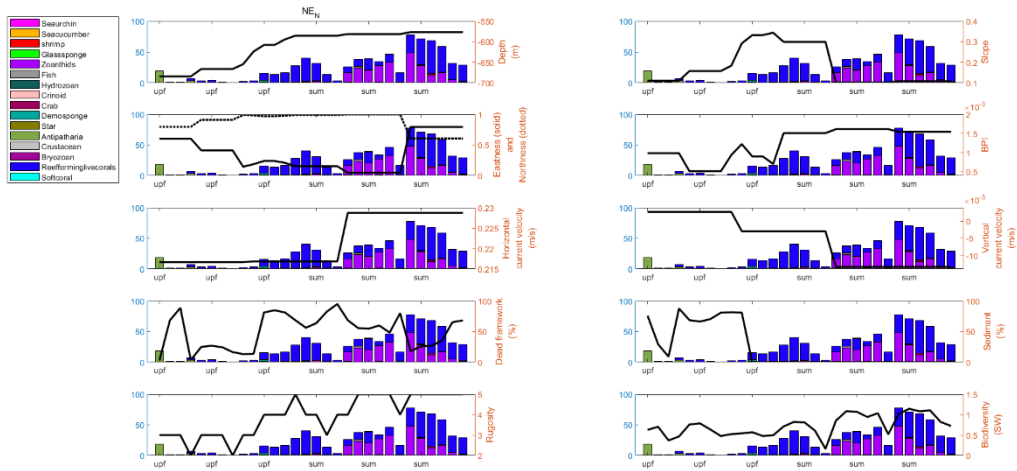

Figure 8. The community assembly and environmental conditions of the transect along the northern flank of Northeast mound. Information regarding the x-axis and y-axis are the same as in figure 2.
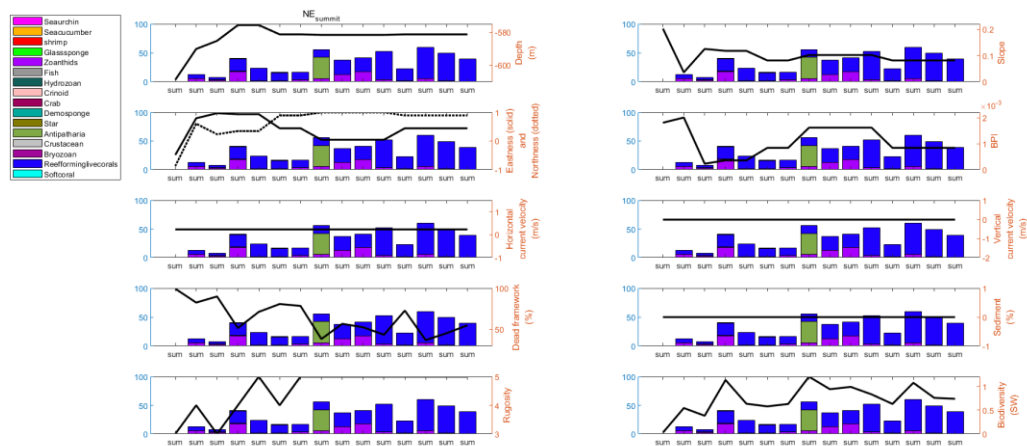
Figure 9. The community assembly and environmental conditions of the transect at the summit of Northeast mound. Information regarding the x-axis and y-axis are the same as in figure 2.

The community assembly on Northeast mound displays a generally increasing richness in live organism coverage from the off-mound area up to the summit, which is similar to that on North mound. The summit is capped with rich reef-forming live corals, which can be up to a maximal coverage of 53%. Other faunal groups with more than 1% coverage at a single site include demosponges, black corals Antipatharia and zoanthids. Zoanthids, which are endemic on Northeast mound compared to North mound and Haas mound, is found of rich coverage at the summit that can be up to 48%. Similar to the North mound, the Northeast mound also has less framework and live organism coverage along the northern flank than along the southern flank.

At the summit of Northeast mound where live organism coverage is found rich, the horizontal current speed ranges approximately from 0.22 m/s to 0.25 m/s, similar with those at the summit of North mound and at the upper flank of Haas mound, where live organism coverage is also relatively rich. The downwelling velocity at the summit of Northeast mound remains close to zero, while BPI ranges from approximately 0.001 to 0.005. Rugosity and biodiversity exhibit association with live organism coverage which is mainly contributed by reef-forming live coral and zoanthid coverage, whereas in sites

at the summit of Northeast mound where live organism coverage can exceed 50%, dead framework coverage is often found below 50%.

Intra-mound community assembly variation

Of all the faunal groups investigated, reef-forming live corals and demosponges generally have the most abundance. The distribution of reef-forming live corals and other sessile organisms including sea urchins, zoanthids, starfish Asteroidea, hydrozoans, and soft corals show highest abundance at the summit, and progressively decreasing down the flank.

Similarly, biodiversity, described by Shannon-Wiener index, is the highest at the summit, but found higher at the lower flank than at the upper flank. Such higher biodiversity at the lower flank than at the upper flank is caused by the relatively even community distribution at the lower flanks and uneven community distribution at the upper flanks; concretely, the upper flanks of NE Haas mound an northern N mound has poor organism coverage compared to their upper flanks. Demosponges and black corals Antipatharia, on the other hand, are most abundant at the upper flank, followed by the summit. Overall, live organism coverage exibits an upward trend from the off-mound area to the summit (figure 10).

Between-class analysis (BCA) by zones summarizes the community assembly variation between off-mound, lower flank, upper flank, and summit areas (figure 11). The largest variation, which in the figure is represented along the horizontal axis, is found between the summit, which covers all the faunal groups but mainly characterized by reef-forming live corals and zoanthids, and the off-mound area, which has barely organism distributed. In addition, the upper flank and the lower flank overlap at a large extent, indicating a similar community assembly, which is mainly characterized by demosponges and black corals Antipatharia.
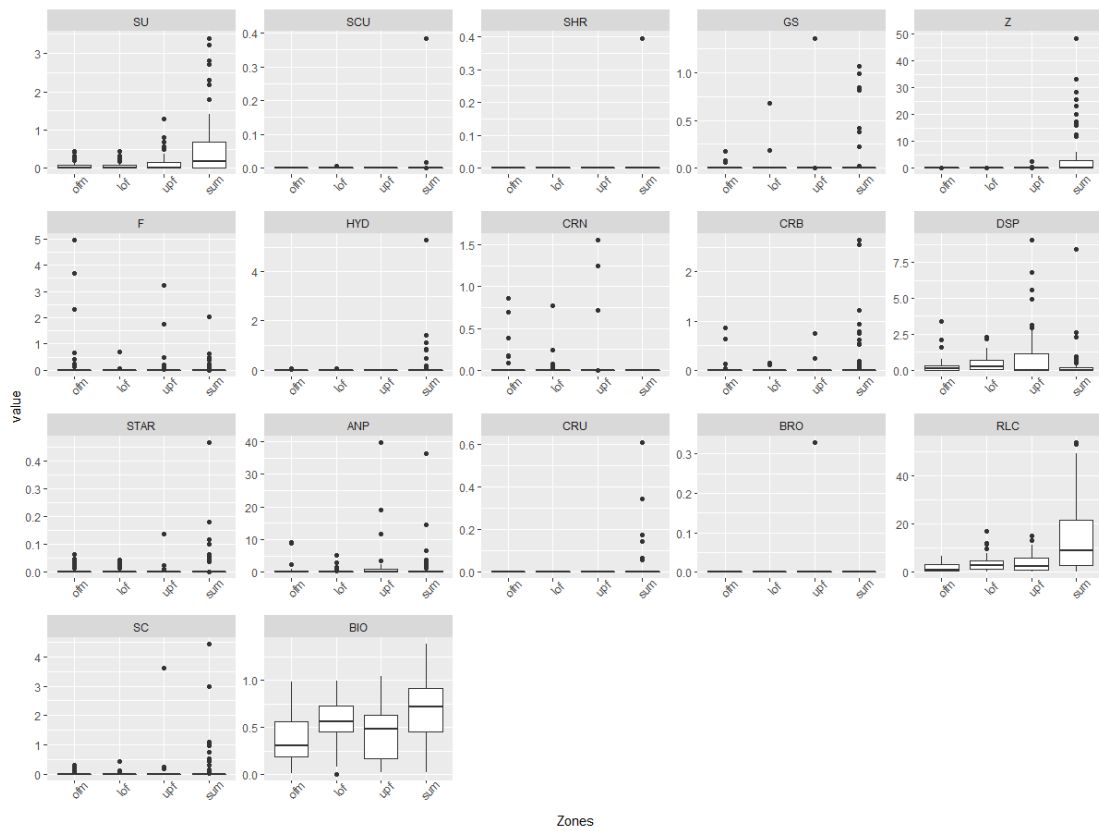
Figure 10. Community assembly and biodiversity at each zone—off-mound area (ofm), lower flank (lof), upper flank (upf), and summit (sum) of all transects. Starting from the top row, from left to right the subfigures refer to sea urchins (SU), sea cucumbers (SCU), shrimps (SHR), glass sponges (GS), zoanthids (Z), fish (F), hydrozoans (HYD), crinoids (CRN), crabs (CRB), demosponges (DSP), starfish Asteroidea (STAR), black corals Antipatharia (ANP), crustaceans (CRU), bryozoans (BRO), reef-forming live corals (RLC), soft corals Gorgonians (SC), and biodiversity in Shannon-Wiener index (BIO), respectively. The y-axes in this figure refer to the percentage of coverage for the corresponding biotic group, except for that of the BIO subfigure, which refers to Shannon-Wiener index.
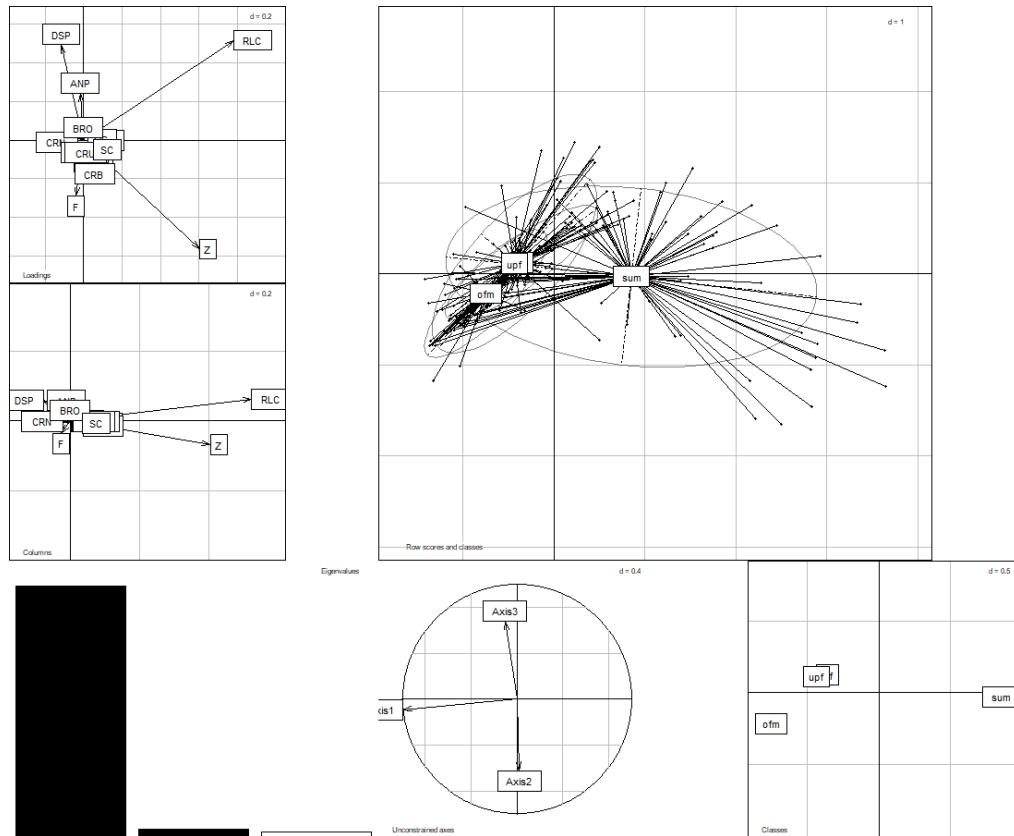
Figure 11. The result of a BCA. It investigates the community assembly variation between the summit, upper flank, lower flank, and off-mound area. The small figure at the top-left refers to the coefficients of the species in the BCA. The small figure under the former one refers to the scores of each species in the feature projection. The bar-plot refers to the eigenvalues. The following small figure on the right shows the projection of the first three axes of the PCA onto the BCA. The small figure at the bottom-right refers to the scores of each group, which in this case is the zone. The main figure (top-right) community includes reef-forming live corals (RLC), zoanthid (Z), dead framework (DF), demosponge (DSP), glass sponge (GS), soft coral (SC), black coral (ANP), crinoid (CRN), bryozoan (BRO), sea urchin (SU), star, hydrozoan (HYD), fish (F), crab (C), and shrimp (S). The first axis refers to the largest variation between classes. Therefore, by integrating the main figure (top right) and the small figure at the top left, we can find to what extent the zones vary from each other, and the community assembly of each zone that characterizes such variation.

Inter-mound community assembly variation

The community assembly and biodiversity of each transect is shown in figure 12. Northest mound has the richest reef-forming live coral distribution, particularly at the summit and the northern flank, with coverage of approximately 21% and 12% respectively. Other faunal groups including zoanthids, sea urchins, and crinoids are also more abundant on this mound, making it a hotspot of high biodiversity, compared to other two mound. Another biodiversity hotspot occur on the western flank of Haas mound, characterized by the abundance of demosponges. Black corals Antipatharia are mainly found on North mound, whose southern flank also witnessed relatively high biodiversity, characterized by comparably even community distribution.

The community assembly variation between transects is summarized with BCA (figure 13). The largest variation occurs between the summit of Northeast mound, the northern flank of Northeast mound, the southern flank of Northeast mound, and other transects. Concretely, the former three transects were all characterized by reef-forming live corals and zoanthids, whereas the transect on the northern flank covered a larger range of faunal groups, which can be explained by that the transect covered more zones than the transect on the summit (figure 1). The transect on the southern flank observes less reef-forming live corals and zoanthids than the one on the summit. The other transects, distributed along the vertical axis of BCA result, display smaller variation and less reef-forming coral and zoanthid coverage than Northeast mound transects. The two transects on Haas mound are mainly characterized by demosponge distribution, while the two transects on North mound are characterized by black corals Antipatharia distribution. Overall, the community assembly variation, both between zones and between transects, are mainly characterized by reef-forming live corals, zoanthids, demosponges and black corals Antipatharia, while other faunal groups do not explain such variation at a large extent.
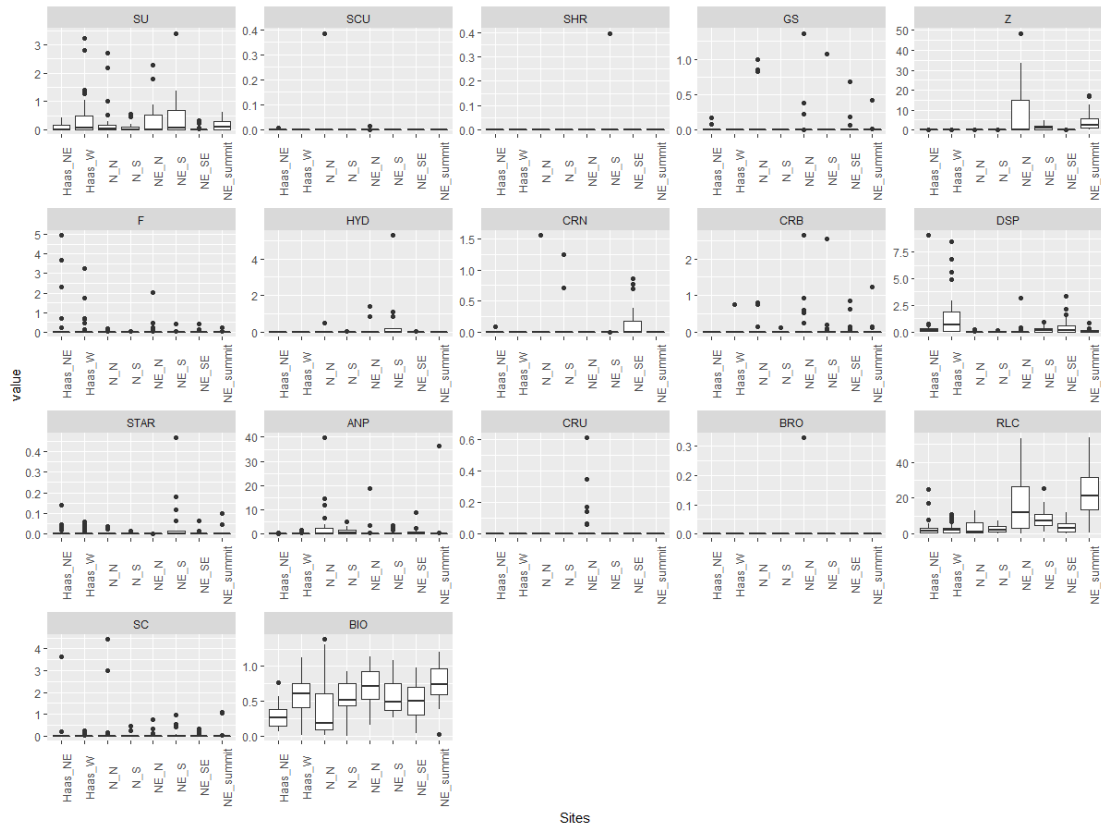
Figure 12. Community assembly and biodiversity at each transect—northeastern flank of Haas mound (Haas_NE), western flank of Haas mound (Haas_W), northern flank of North mound (N_N), southern flank of North mound (N_S), northern flank of Northeast mound (NE_N), southern flank of Northeast mound (NE_S), southeastern flank of Northeast mound (NE_SE), and the summit of Northeast mound (NE_summit). Again, the y-axes in this figure refer to the percentage of coverage for the corresponding biotic group, except for that of the BIO subfigure, which refers to Shannon-Wiener index.
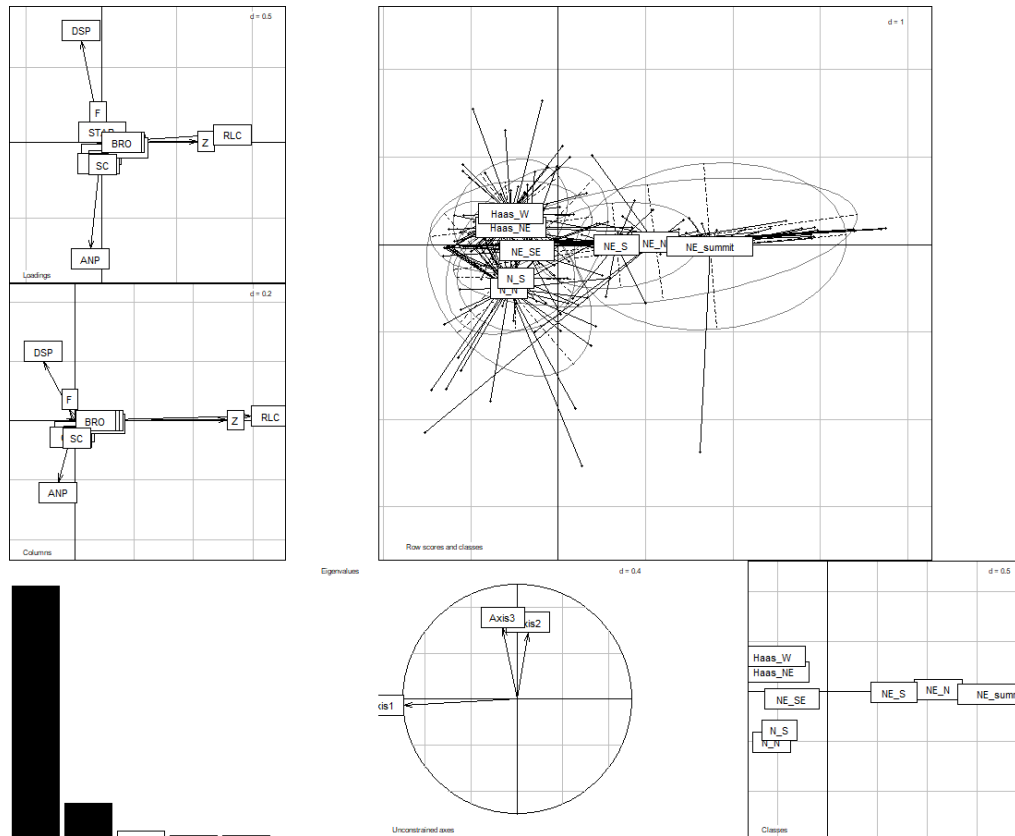
Figure 13. The result of BCA. It investigates the community assembly variation between transects. The layout and the way of interpretation are the same as those of figure 11.

3.2   Environmental variables

Topographic features—slope, eastness, northness, BPI, and rugosity, and hydrodynamic features—horizontal current velocity, downwelling velocity and upwelling velocity, together with sediment exposure rate and the dead framework coverage, are depicted in figure 14.
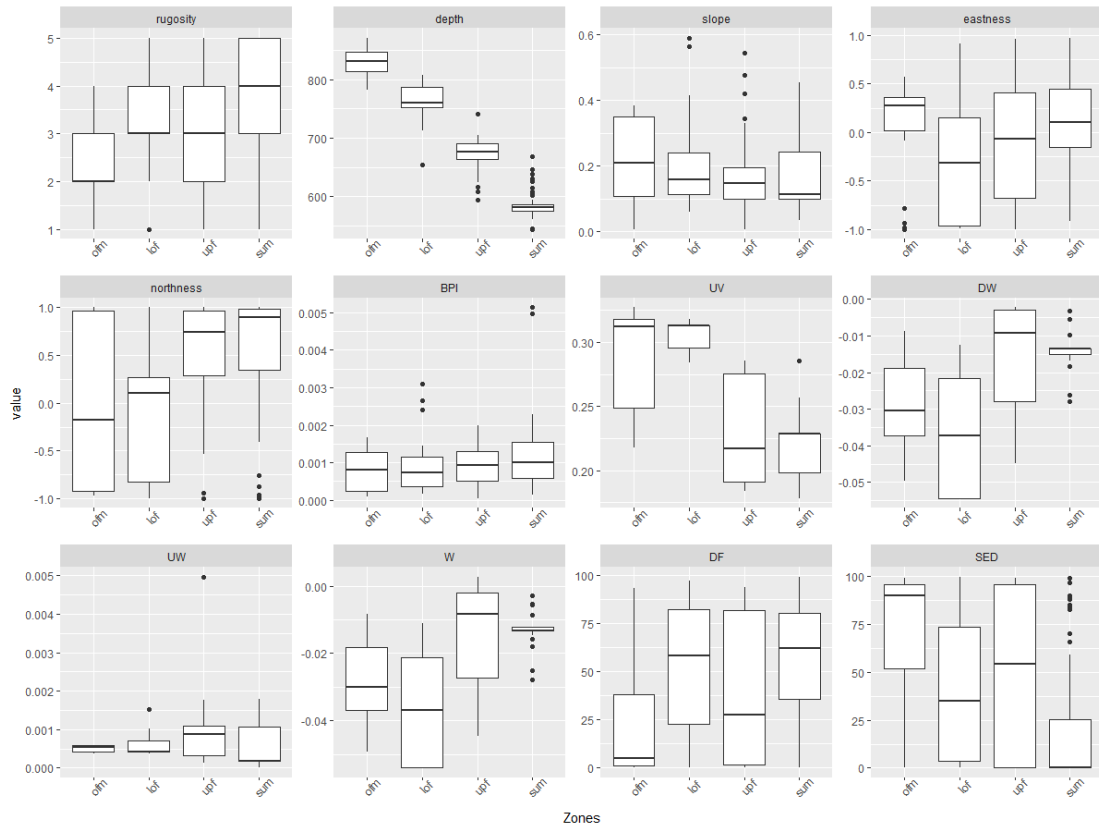
Figure 14. Topographical and hydrodynamic conditions, and sediment exposure rate and dead framework coverage at each zone—off-mound area (ofm), lower flank (lof), upper flank (upf), and summit (sum) of all transects. Starting from the top row, from left to right the subfigures refer to rugosity in habitat assessment score, depth in meter, slope, eastness, northness, BPI, horizontal current velocity (UV) (m/s), downwelling velocity (DW) (m/s), upwelling velocity (UW) (m/s), dead framework coverage in percentage, and sediment coverage in percentage.

The summit areas are generally characterized by high rugosity, low depth, gentle slope, high BPI, low horizontal current velocity, low downwelling and upwelling velocity, medium deadframework coverage, and low sediment exposure. The flanks, including upper flanks and lower flanks, have similar seabed conditions, which are medium rugosity, medium slope, high dead framework coverage, and medium sediment exposure, while the BPI of lower flanks is generally the lowest and the BPI of upper

flanks is the second highest of all zones. In addition, hydrodynamic conditions between upper and lower flanks varied at a large extent. Model shows high horizontal current velocity, high downwelling velocity, and medium upwelling velocity at lower flanks, while it also shows low horizontal current velocity, low downwelling but high upwelling velocity at upper flanks. The general environmental conditions at the off-mound area were low rugosity, high depth, steep slope, medium BPI, high current velocity, medium upwelling and downwelling velocity, low dead framework coverage, and high sediment exposure.
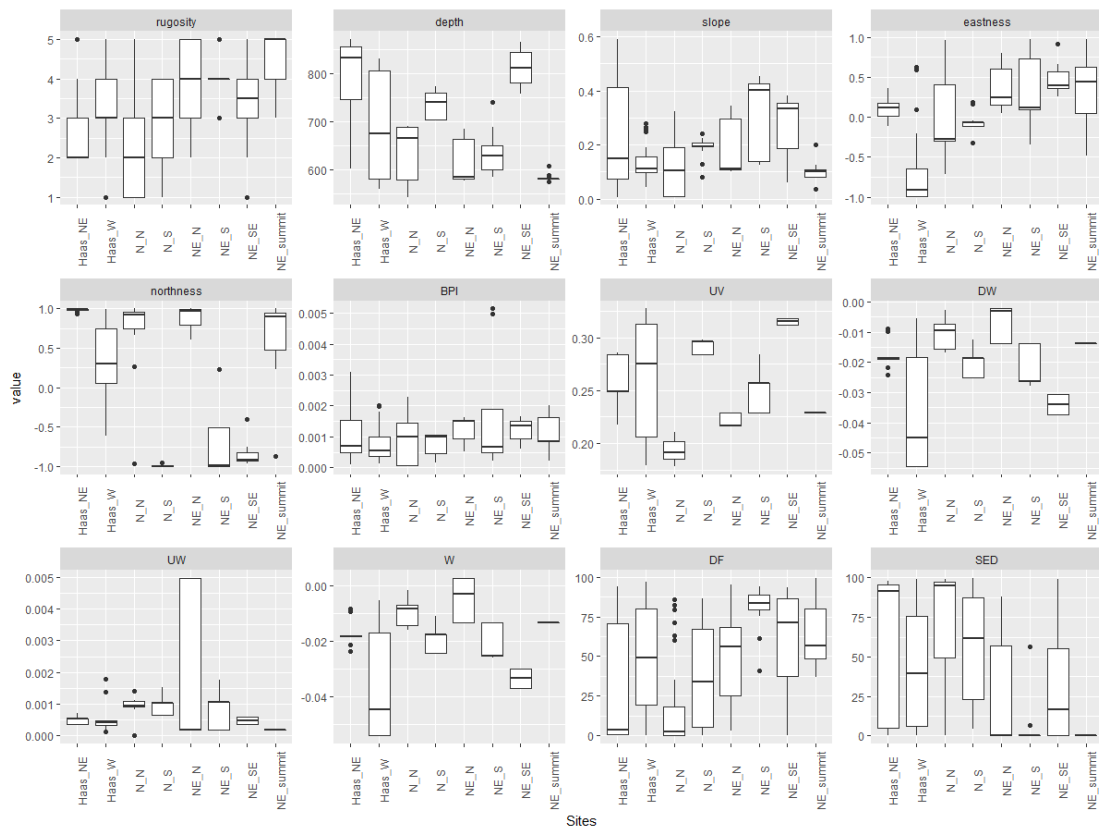
Figure 15. Topographical and hydrodynamic conditions, and sediment exposure rate and dead framework coverage at each transect—northeastern flank of Haas mound (Haas_NE), western flank of Haas mound (Haas_W), northern flank of North mound (N_N), southern flank of North mound (N_S), northern flank of Northeast mound (NE_N), southern flank of Northeast mound (NE_S), southeastern flank of Northeast mound (NE_SE), and the summit of Northeast mound (NE_summit). The *y*-axes of the subfigures denote the same as those of figure 14.

The environmental variables per transect are shown in figure 15. Transects on Northeast mound, where biodiversity hotspots are witnessed, are commonly characterized by high rugosity, high dead framework coverage, and low sediment exposure. Among these transects, the ones at the northern flank and the summit, with higher reef-forming live coral coverage and biodiversity, have gentler slopes, lower horizontal current velocity, and lower downwelling velocity, while the BPI at the northern flank of Northeast mound is higher than that at the summit of the same mound. The western flank of Haas mound, another biodiversity hotspot characterized by demosponge distribution, has medium rugosity, gentle slope, low BPI, high horizontal current velocity, high downwelling velocity, low upwelling, medium dead framework coverage and medium sediment exposure. The northeastern flank of Haas mound, however, has very different environmental conditions compared to the western flank, with lower rugosity, horizontal current velocity, downwelling velocity, and dead framework coverage, but higher slope steepness, BPI, upwelling velocity, and sediment exposure. North mound, characterized by black corals Antipatharia distribution, also has a large variation between the environmental conditions of northern flank and southern flank. Covering the upper flank and the summit of the mound, the transect at the northern flank of North mound is characterized by lower rugosity, depth, slope, horizontal current velocity, downwelling velocity, and dead framework coverage than the transect at the southern flank, which covers the lower flank and the upper flank (figure 1).

3.3 Co-inertia analysis

The result of co-inertia analysis reveals the relationship between environmental variables and species coverage (figure 16). The environmental data and species data have 40% agreement ($RV = 0.40$) on a high significant level ($P = 0.0001$). Reef-forming live corals are found to have strong positive correlation with rugosity, BPI,

dead framework coverage, and negative correlation with upwelling and sediment exposure. Non-reef-forming corals, i.e. black corals Antipatharia and soft corals Alcyonacea (i.e. soft corals), more densely distributed at the northern and eastern flanks than at the southern and western flanks, are found positively correlated with BPI and downward current speed, while negatively correlated with horizontal current velocity, and slope. Zoanthids, which tend to co-exist with reef-forming live corals as previously shown, do not share very similar environmental preference with them, but instead their corresponding environment conditions largely overlap the ones of non-reef-forming corals. Demosponges, meanwhile, mainly occur at sites with environment to the opposite of what non-reef-forming corals and zoanthids have strong correlation, including high horizontal current velocity, high dead framework coverage, steep slopes, and low vertical current speed.
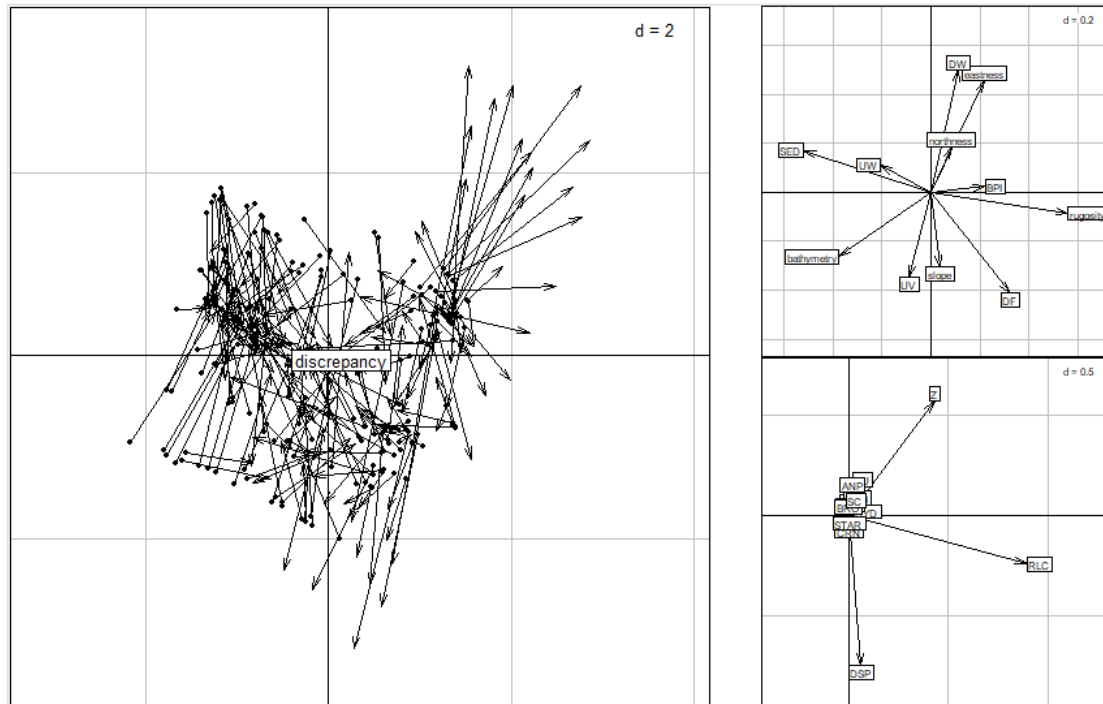
Figure 16. The result of co-inertia analysis ($P = 0.0001$). The two small figures on the right denote the coefficients of the environmental variables (top) and species coverage (bottom) in the co-inertia. If an environmental variable and a species appear at similar relative positions on the coordinate systems, they have a positive correspondence. The big figure on the left denotes the discrepancy between the environmental variables and the species coverage per site. The dot refers to the site described by environmental variables; the end of the arrow refers to the site described by species coverage. Therefore, a shorter arrow represents a better correspondence between environmental variables and species composition of a single site.

Table 4. Summary of important faunal group distribution and their correlated environmental factors

Faunal groups	Preferred zone	Preferred mound	Correlated hydrodynamic conditions	Correlated topographical conditions
Reef-forming live corals	Summit	Northeast mound	Low upwelling	High BPI, high rugosity, high dead framework coverage, low sediment exposure
Antipatharia	upper & lower flank, summit	North mound	High downwelling, low horizontal current velocity	Northern & eastern flank, low slope steepness, high BPI
Soft corals	upper & lower flank, summit	Northeast mound	High downwelling, low horizontal current velocity	Northern & eastern flank, low slope steepness, high BPI
Zoanthids	summit	Northeast mound	High downwelling, low horizontal current velocity	Northern & eastern flank, low slope steepness, high BPI
Demosponges	upper & lower flank, summit	Haas mound	High horizontal current velocity, low downwelling	Southern & western flank, high slope steepness, high dead framework coverage

4 Discussion

The results indicate that both the intra-mound variation and the inter-mound variation of community assembly, depicted by the variation between zones and between dives respectively, are mainly characterized by the distribution of reef-forming live corals, zoanthids, demosponges, and black corals Antipatharia. Live reef forming corals and zoanthids occurred more in summit areas but exhibit a relatively equal distribution along the upper flank, lower flank, and the off-mound area. Demosponges and black corals Antipatharia concentrate at lower topographical positions, particularly at the upper flank, but their coverage was generally lower than reef-forming live corals. The off-mound area, the lower flank, and the upper flank share similar community composition, with very limited coverage of live megafauna, whereas dead framework coverage is higher at the upper flank and the summit, while sediment exposure is the highest at the off-mound area. Among all the transects studied, the NE mound contained highest concentration/density/abundance of reef-forming live corals and zoanthids, particularly at its summit and the northern flank. Demosponges mainly occur along the transects at Haas mound, while black corals Antipatharia concentrate along the transects at North mound.

It has been hypothesized that seamounts can function as ecological islands with high level endemism in community composition (Roberts et al., 2009). However, our study shows that generally, transects from the same mound, though along flanks in different directions and positions, display similar community assembly, which implies that ecological islands emerge on the mound scale as well. Unfortunately, our results fail to explain such mound-scale ecological islands with the "environmental control theory", because the environmental conditions between different flanks of the same mound vary greatly in our study. We hypothesize that, the occurrence of endemic faunal groups on a mound is the result of random effect, whereas the lack of hydrodynamic connectivity between mounds obstructs the diffusion of their larvae to other mounds.

Environmental factors that exhibit correlation with the coverage of faunal groups

are summarized in table 4. Although reef-forming live corals and zoanthids exhibit similar distribution, their correlated environmental features are highly distinct. Reef-forming live corals are associated with high BPI, high rugosity, high dead framework coverage, and low sediment exposure, but do not have high correlation with slope steepness, slope orientation (i.e. northness and eastness), downwelling, and horizontal current speed. Zoanthids, with denser occurrence along the northern and eastern flanks, display positive correlation with BPI and downwelling, but negative correlation with slope and horizontal current velocity. Also, demosponges and black corals Antipatharia show similar distribution but have distinct correlated environmental features. Both groups occur mainly at the upper flank of the transects. Black corals Antipatharia, mainly distributed along the northern and eastern flanks, are associated with high BPI, high downwelling, and low horizontal current velocity, whereas demosponges have positive correlation with slope steepness, dead framework coverage, and horizontal current velocity, but negative correlation with downwelling. Such similarity in distribution and distinction in associated environmental factors provide detailed information regarding the high discrepancy (long arrows) in figure 16. A potential explanation is that for each site (i.e. image layer), all environmental variables and faunal groups coverage were tested, but a faunal group may be only correlated with a part of the investigated environmental factors, whereas other environmental factors may not be linearly correlated or relevant. For example, reef-forming live corals and zoanthids are both associated with high BPI, while horizontal current velocity and downwelling, according to our results, do not correlate with reef-forming live corals. Another potential explanation is that, in this study, we only tested the effect of seabed topography and hydrodynamics, whereas there may be other important factors that were not included, e.g. biochemical factors (Barbosa et al., 2020) and biotic factors, e.g. competition between black corals Antipatharia and reef-forming live corals, as they are both passive suspension feeder, directly capturing particulate organic matter with their tentacles (Lewis, 1978).

Rugosity has a high agreement with reef-forming live coral coverage, but this

correlation is probably because the reef-forming corals increase the rugosity by forming reef structures. Rugosity could be an explanatory factor for other faunal groups, as it increases the habitat heterogeneity, thus supporting the settlement and providing refuge for other organisms (Price et al., 2019). This also aligns with the finding that, sites with high rugosity, high dead framework coverage and low sediment exposure, are associated with high biodiversity. Meanwhile, other environmental factors, i.e. hydrodynamics, slope steepness, slope orientation, and BPI, can serve as explanatory factors of the community assembly, because they were modeled or calculated without the impact of live organisms.

Implications of topography-community correlations

Compared to North mound and Haas mound, Northeast mound has the smallest size but shows highest reef-forming coral abundance, mainly distributed at its summit, whereas Haas mound, the largest mound of the three, has barely reef-forming corals distributed at its summit. These findings imply the spatial variation of cold-water coral community distribution relating to the mound size, that, species are likely to concentrate at the summit and/or the upper flank of smaller mounds, but mainly at the upper flank of larger mounds. This implication further supports the hypothesis of Cyr et al. (2016) that Haas mound could have reached its stable state in height, while smaller mounds, e.g. Northeast mound and North mound, with reef-forming live corals capping on their summits, still have the potential of vertical growth.

Reef-forming live coral distribution shows positive correlation with BPI, which is in line with previous studies (De Clippele et al., 2017; Diesing & Thorsnes, 2018; Sudahl et al., 2020). As BPI refers to the terrain curvature (Wilson et al., 2007), the summit often has the largest BPI value compared to other zones of a mound, which corresponds to that the summit is often characterized by abrupt changes of the slope. Therefore, a positive correlation between the coverage of most reef community fauna

and BPI implies a dense distribution of these faunal groups and high biodiversity at the summit. However, studies that investigate the relationship between BPI and local hydrodynamics so far remain limited. Therefore, the mechanisms lying in the BPI-coral correlation are still poorly learnt.

BPI in this study was calculated through discretization. However, at sites with abundant reef-forming live coral distribution, the maximum BPI in this study was approximately 0.002, while the value in relevant studies can reach 7 (De Clippele et al., 2017; Diesing & Thorsnes, 2018; Sudahl et al., 2020), showing a large discrepancy. Method of BPI calculation is expected to be a key factor, as BPI derived in BTM/ArcGIS is a very common algorithm used by numerous studies (Weiss, 2011). The general difference between the BTM/ArcGIS method and our method of BPI calculation is that the BTM/ArcGIS method calculates the curvature of the terrain, while our method calculates the derivative of the slope angle, referring to the its changing rate. Nevertheless, as both methods calculate the relative position of the location compared to its surroundings, the trend should be similar.

In this study, slope steepness is not linearly correlated with the distribution of faunal groups except for demosponges. The relationship between slope steepness and reef-forming live corals is controversial in other studies, as Sudahl et al. (2020) found *L. pertusa* and two soft coral Alcyonacea species had preference over moderate sloping terrains, while Rengstorf et al. (2014) simulated an increase of reef-forming live coral presence probability with increasing slope. According to Kunze (2004), slope is closely related to hydrodynamics, and our results indeed show a similar relationship between fauna and slope as between fauna and hydrodynamics, which will be subsequently discussed.

Implications of hydrodynamics-community correlations

Our results indicate that reef-forming live coral coverage show no linear correlation

with horizontal current velocity or downward current speed but are negative correlated with upward current speed. These results with previous studies which found an association between reef-forming live coral presence and intensified benthic currents and downwelling (Mohn et al., 2014; Davies et al., 2009). Mohn et al. (2014) indicated that tidal amplification induced by bottom trapped waves, plus rapid downwelling, serve as important mechanisms to transport surface production in the Rockall Trough to the reef community fauna in the deep water. However, amplified currents are not always beneficial, because they can reduce the food capture capability of corals by sweeping their tentacles and thus limiting their feeding area (Purser et al., 2010). Furthermore, L. pertusa has/showed an optimal food capture at current velocity ($<$ $7\ cm/s$) in a laboratory setting (Orejas et al. 2016). Therefore, we hypothesize that reef community occurrence in the deep water do not monotonically correlate with the benthic current velocity, but there should be a range of optimal benthic current velocity that can guarantee both ample food transport from surface production and effective food captured by corals and other suspension feeders.

Demosponges display strong positive correlation with horizontal current velocity. It was presumed that coral reefs would occur at environments with high bottom current velocity and thrive at the outer edge of dead framework, because corals, which are passive feeders, may rely on strong currents for food transport more than demosponges, which can actively pump the water (Mortensen et al., 2008). However, our result shows that demosponges are more reliant on high current velocity than corals. A possible explanation is that, sponges require high energy consumption, i.e. $>$ 28% of their metabolism, when pumping water, and they were therefore hypothesized to make use of current-induced flows (Leys et al., 2011; Vogel, 1977). At higher ambient current velocity, sponges generally exhibit an increase of excurrent velocity, a decrease of oxygen removal rate, and stable filtration-to-respiration ratio. This implies that, under amplified ambient currents, sponges constrict their oscula, controlling the water pumping and leading to a reduction of energy consumption (Ludeman et al., 2017). Although it is still controversial that whether sponges make use of current-induced flow

to save energy, they have shown well adaptation to environment with high current velocity.

Uncertainties

Uncertainties of our study lie in (1) the limit of coverage calculation, (2) the limit of 'snapshot' methodology, and (3) the possibility of human impact.

As faunal group abundance in this study was calculated through the percentage of coverage, it presumed that all species were distributed on a two-dimensional plane, instead of a three-dimensional framework. Hence, organisms, particularly demosponges encrusting in the framework would be overlooked, causing a underestimation of the resulted species abundance.

Given the difficulty of inspecting the process of community colonization, this study was based on a 'snapshot' of the community assembly. In this case, the entire mound development can be regarded as a "quasi-equilibrium" process, and the current community assembly represents the equilibrium between species and the environment. However, as the environmental conditions may be favored by various species, the ones with certain strategies would then be more likely to outcompete others, leading to an alternation of species dominance. For instance, coral reefs at shallower depths may at first be colonized by fast-growing organisms, e.g. tunicates and bryozoans; but then, large colonial organisms, if successfully established, would soon occupy the space and outgrow the former species, thus becoming dominant at the local scale (Birkeland, 1977). This theory can explain the lack of tunicates and bryozoan presence in the present study, but the potential competition process is difficult to investigate.

The validity of the environment-fauna relationship can be greatly affected by human impact, e.g. fishery, deep-sea mining, and hydrocarbon exploration (Ragnarsson et al., 2017). Commercial fishery of orange roughly fish in Northeast Atlantic has been

popular since late 1970s and fishery activities in Rockall area were also recorded (Foley et al., 2011; Charuau et al., 1995). Bottom trawling, a major fishing approach delivering more than 20% of the global fish catch, has long been a severe threat to deep-sea ecosystems, damaging habitats and killing organisms (Kelleher, 2005; Wheeler et al., 2005). Consequently, it is possible that the reef community assembly has been altered or even diminished by bottom trawling, and the environment and the current faunal composition may therefore not correspond to each other, leading to discrepancies in the investigation of the environment-fauna relationship. Moreover, coral recovery is a slow process, during which different succession stages may take place (Roberts et al., 2009; Birkeland, 1977); these processes further increase the uncertainties that whether the current community assembly serves as good representative of the environmental conditions.

Research outlook

Future research is suggested to delve more into the cold-water coral reef biochemistry, specifically how food particles are transported to cold-water coral reefs and how they circulate within and/or between the community on a regional scale. Since the major food transport pathways are different from place to place, the corresponding environmental impact factors that determine the community distribution can be accordingly different. For instance, De Clippele et al. (2017) found that depth could be a key factor of the coral-capped carbonate mound distribution on Mingulay reef complex, because the corals there highly rely on the tidal downwelling that transports food from the surface production and thus the deeper the location is, the more difficult it receives food particles. However, depth is not an important factor in our study, as the summit of Northeast mound is deeper than the summit of Haas mound, the former one has higher coral abundance, implying a different major food transport mechanism in southeastern Rockall area.

Another future research prospect is the niche study of non-reef-forming corals and other common non-coral organisms. Since we have found mound-scale endemic species which so far cannot be explained, a thorough niche study or habitat suitability study of these species can shed light on the factors that govern their distribution, enabling a more in-depth understanding of the cold-water coral reef ecosystem.

5 Conclusion

In summary, in this study, we investigated the linkage between community assembly and environmental variables, i.e. topography, hydrodynamics, and local environmental determinants such as rugosity, sediment, and dead coral framework. Our results show that reef-forming corals, zoanthids and non-reef-forming corals (i.e. black corals Antipatharia and soft corals Alcyonacea) are positively correlated with BPI, which is often found relatively high values at the summit; reef-forming corals do not have correlation with horizontal current velocity, whereas non-reef-forming corals and zoanthids are negatively correlated with horizontal current velocity, which is because corals rely on amplified current to transport food, but cannot effectively capture food particles in high current speed; demosponges display strong correlation with slope steepness and horizontal current velocity, implying a mechanism for them to save energy when pumping water.

We further investigated how this linkage differed between mounds and within mounds, to get insight into whether there are general patterns that are consistent on all mounds, as compared to differences that exist between individual mounds. We have found a spatial variation of cold-water coral reef community distribution in relation to mound size, that the community generally concentrates at the summit of smaller mounds, while at the upper flank of larger mounds, implying a potential of vertical growth for small mounds and a steady state of that for larger mounds. Future research is suggested to focus more on the biochemical studies related to cold-water coral reefs on regional scale, and the niche studies of mound-scale endemic species, to obtain more

insights regarding the conservation of deep-water ecosystems under climate change.

6 References

Barbosa, R. V., Davies, A. J., & Sumida, P. Y. G. (2020). Habitat suitability and environmental niche comparison of cold-water coral species along the Brazilian continental margin. Deep Sea Research Part I: Oceanographic Research Papers, 155, 103147.

Birkeland, C. (1977). The importance of rate of biomass accumulation in early succession stages of benthic communities to the survival of coral recruits. In Proc. 3rd Int. Coral Reef Symp. (pp. 16-21).

Cacchione, D. A., Pratson, L. F., & Ogston, A. S. (2002). The shaping of continental slopes by internal tides. Science, 296(5568), 724-727.

Charuau, A., Dupouy, H., & Lorance, P. (1995). French exploitation of the deep-water fisheries of the North Atlantic. In Deep-water fisheries of the North Atlantic oceanic slope (pp. 337-356). Springer, Dordrecht.

Chessel, D., Dufour, A. B., & Thioulouse, J. (2004). The ade4 package-I-One-table methods. R news, 4(1), 5-10.

Cyr, F., van Haren, H., Mienis, F., Duineveld, G., & Bourgault, D. (2016). On the influence of cold-water coral mound size on flow hydrodynamics, and vice versa. Geophysical Research Letters, 43(2), 775-783.

Davies, A. J., Duineveld, G. C., Lavaleye, M. S., Bergman, M. J., van Haren, H., & Roberts, J. M. (2009). Downwelling and deep-water bottom currents as food supply mechanisms to the cold-water coral Lophelia pertusa (Scleractinia) at the Mingulay Reef Complex. Limnology and Oceanography, 54(2), 620-629.

Davies, A. J., & Guinotte, J. M. (2011). Global habitat suitability for framework-forming cold-water corals. *PloS one*, *6*(4), e18483.

De Clippele, L. H., Gafeira, J., Robert, K., Hennige, S., Lavaleye, M. S., Duineveld, G. C. A., ... & Roberts, J. M. (2017). Using novel acoustic and visual mapping tools to predict the small-scale spatial distribution of live biogenic reef framework in cold-water coral habitats. Coral Reefs, 36(1), 255-268.

De Goeij, J. M., Van Oevelen, D., Vermeij, M. J., Osinga, R., Middelburg, J. J., de Goeij, A. F., & Admiraal, W. (2013). Surviving in a marine desert: the sponge loop retains resources within coral reefs. Science, 342(6154), 108-110.

Diesing, M., & Thorsnes, T. (2018). Mapping of cold-water coral carbonate mounds based on geomorphometric features: an object-based approach. Geosciences, 8(2), 34.

Dolan, M. F., Grehan, A. J., Guinan, J. C., & Brown, C. (2008). Modelling the local distribution of cold-water corals in relation to bathymetric variables: Adding spatial context to deep-sea video data. Deep Sea Research Part I: Oceanographic Research Papers, 55(11), 1564-1579.

Dustan, P., Doherty, O., & Pardede, S. (2013). Digital reef rugosity estimates coral reef habitat complexity. PloS one, 8(2), e57386.

Foley, N. S., van Rensburg, T. M., & Armstrong, C. W. (2011). The rise and fall of the Irish orange roughy fishery: an economic analysis. Marine Policy, 35(6), 756-763.

Freiwald, A. (2002). Reef-forming cold-water corals. In Ocean margin systems (pp. 365-385). Springer, Berlin, Heidelberg.

Freiwald, A. (2011). Cold-water coral reefs. Encyclopedia of modern coral reefs: structure, form and process, 225-229.

Gage, J. D., & Tyler, P. A. (1991). Deep-sea biology: a natural history of organisms at the deep-sea floor. Cambridge University Press.

Gratwicke, B., & Speight, M. R. (2005). The relationship between fish species richness, abundance and habitat complexity in a range of shallow tropical marine habitats. Journal of fish biology, 66(3), 650-667.

Guinan, J., Grehan, A. J., Dolan, M. F., & Brown, C. (2009). Quantifying relationships between video observations of cold-water coral cover and seafloor features in Rockall Trough, west of Ireland. Marine Ecology Progress Series, 375, 125-138.

Jones, C. G., Lawton, J. H., & Shachak, M. (1994). Organisms as ecosystem engineers. In Ecosystem management (pp. 130-147). Springer, New York, NY.

Iampietro, P., & Kvitek, R. (2002, July). Quantitative seafloor habitat classification using GIS terrain analysis: Effects of data density, resolution, and scale. In Proceedings of the 22nd Annual ESRI User Conference (pp. 8-12).

Kelleher, K. (2005). Discards in the world's marine fisheries: an update (Vol. 470). Food & Agriculture Org.

Kenyon, N. H., Akhmetzhanov, A. M., Wheeler, A. J., van Weering, T. C., de Haas, H., & Ivanov, M. K. (2003). Giant carbonate mud mounds in the southern Rockall Trough. Marine Geology, 195(1-4), 5-30.

Kunze, E., & Smith, S. L. (2004). The role of small-scale topography in turbulent mixing of the global ocean. Oceanography, 17(1), 55-64.

Lewis, J. B. (1978). Feeding mechanisms in black corals (Antipatharia). Journal of Zoology, 186(3), 393-

396.

Leys, S. P., Yahel, G., Reidenbach, M. A., Tunnicliffe, V., Shavit, U., & Reiswig, H. M. (2011). The sponge pump: the role of current induced flow in the design of the sponge body plan. PloS one, 6(12).

Ludeman, D. A., Reidenbach, M. A., & Leys, S. P. (2017). The energetic cost of filtration by demosponges and their behavioural response to ambient currents. Journal of Experimental Biology, 220(6), 995-1007.

Lundblad, E. R., Wright, D. J., Miller, J., Larkin, E. M., Rinehart, R., Naar, D. F., ... & Battista, T. (2006). A benthic terrain classification scheme for American Samoa. Marine Geodesy, 29(2), 89-111.

Mienis, F., De Stigter, H. C., White, M., Duineveld, G., De Haas, H., & Van Weering, T. C. E. (2007). Hydrodynamic controls on cold-water coral growth and carbonate-mound development at the SW and SE Rockall Trough Margin, NE Atlantic Ocean. Deep Sea Research Part I: Oceanographic Research Papers, 54(9), 1655-1674.

Mohn, C., Rengstorf, A., White, M., Duineveld, G., Mienis, F., Soetaert, K., & Grehan, A. (2014). Linking benthic hydrodynamics and cold-water coral occurrences: A high-resolution model study at three cold-water coral provinces in the NE Atlantic. Progress in Oceanography, 122, 92-104.

Morgan, N. B., Goode, S., Roark, E. B., & Baco-Taylor, A. (2019). Fine scale assemblage structure of benthic invertebrate megafauna on the North Pacific seamount Mokumanamana. Frontiers in Marine Science, 6, 715.

Mortensen, P. B., Buhl-Mortensen, L., Gebruk, A. v., & Krylova, E. M. (2008). Occurrence of deep-water corals on the Mid-Atlantic Ridge based on MAR-ECO data. Deep-Sea Research Part II: Topical Studies in Oceanography, 55(1–2), 142–152. https://doi.org/10.1016/j.dsr2.2007.09.018

Orejas, C., Gori, A., Rad-Menéndez, C., Last, K. S., Davies, A. J., Beveridge, C. M., ... & Roberts, J. M. (2016). The effect of flow speed and food size on the capture efficiency and feeding behaviour of the cold-water coral Lophelia pertusa. Journal of Experimental Marine Biology and Ecology, 481, 34-40.

Price, D. M., Robert, K., Callaway, A., Hall, R. A., & Huvenne, V. A. (2019). Using 3D photogrammetry from ROV video to quantify cold-water coral reef structural complexity and investigate its influence on biodiversity and community assemblage. Coral Reefs, 38(5), 1007-1021.

Purser, A., Larsson, A. I., Thomsen, L., & van Oevelen, D. (2010). The influence of flow velocity and food concentration on Lophelia pertusa (Scleractinia) zooplankton capture rates. Journal of Experimental Marine Biology and Ecology, 395(1-2), 55-62.

Ragnarsson, S. Á., Burgos, J. M., Kutti, T., van den Beld, I., Egilsdóttir, H., Arnaud-Haond, S., & Grehan, A. (2017). The impact of anthropogenic activity on cold-water corals. Marine Animal Forests, 1-35.

Rengstorf, A. M., Mohn, C., Brown, C., Wisz, M. S., & Grehan, A. J. (2014). Predicting the distribution of deep-sea vulnerable marine ecosystems using high-resolution data: Considerations and novel

approaches. Deep Sea Research Part I: Oceanographic Research Papers, 93, 72-82.

Rix, L., De Goeij, J. M., Mueller, C. E., Struck, U., Middelburg, J. J., Van Duyl, F. C., ... & Van Oevelen, D. (2016). Coral mucus fuels the sponge loop in warm-and cold-water coral reef ecosystems. Scientific reports, 6(1), 1-11.

Roberts, J. M. Shipboard Party, 2013. RRS James Cook 073 Cruise Report.

Roberts, J. M., Wheeler, A., Freiwald, A., & Cairns, S. (2009). Cold-water corals: the biology and geology of deep-sea coral habitats. Cambridge University Press.

Soetaert, K., Mohn, C., Rengstorf, A., Grehan, A., & Van Oevelen, D. (2016). Ecosystem engineering creates a direct nutritional link between 600-m deep cold-water coral mounds and surface productivity. Scientific reports, 6, 35057.

Team, R. C. (2019). R: a language and environment for statistical computing. R Foundation for Statistical Computing, Austria.

Thioulouse, J., Dray, S., Dufour, A. B., Siberchicot, A., Jombart, T., & Pavoine, S. (2018). Multivariate analysis of ecological data with ade4. New York, Dordrecht, London, Heidelberg: Springer.

van Weering, T. C., De Haas, H., De Stigter, H. C., Lykke-Andersen, H., & Kouvaev, I. (2003). Structure and development of giant carbonate mounds at the SW and SE Rockall Trough margins, NE Atlantic Ocean. Marine Geology, 198(1-2), 67-81.

Vogel, S. (1977). Current-induced flow through living sponges in nature. Proceedings of the National Academy of Sciences, 74(5), 2069-2071.

Weiss, A. (2001, July). Topographic position and landforms analysis. In Poster presentation, ESRI user conference, San Diego, CA (Vol. 200).

Wheeler, A. J., Bett, B. J., Billett, D. S. M., Masson, D. G., & Mayor, D. J. (2005). The impact of demersal trawling on northeast Atlantic deepwater coral habitats: the case of the Darwin Mounds, United Kingdom. In American Fisheries Society Symposium (Vol. 41, pp. 807-818). American Fisheries Society.

Wilson, M. F., O'Connell, B., Brown, C., Guinan, J. C., & Grehan, A. J. (2007). Multiscale terrain analysis of multibeam bathymetry data for habitat mapping on the continental slope. Marine Geodesy, 30(1-2), 3-35.